SEPARATION OF BULK DIFFUSION LENGTH & BACK SURFACE RECOMBINATION VELOCITY BY IMPROVED IQE-ANALYSIS

M. Spiegel, B. Fischer, S. Keller, E. Bucher,
University of Konstanz, Faculty of Physics, P.O. Box X916, D-78457 Konstanz, Germany
Email: Markus.Spiegel@uni-konstanz.de

ABSTRACT

Key parameters for the quantification of minority carrier recombination in solar cells are the effective bulk diffusion length, the bulk diffusion length and the back surface recombination velocity. As wafer thickness decreases and bulk quality increases the simultaneous determinat-ion of these parameters gains importance for cell process optimization in PV industry. Methods for obtaining these parameters have been described in literature, such as the linear approximation on the inverse IQE vs. light penetration depth. We will formulate the limitations of this approach using numerically and experimentally determined IQE-data. The ambiguity of the older approach is solved by an improved equation, making it possible to obtain these parameters from a fit on the IQE within 820 - 940 nm. In addition an equation incl. the loss in the emitter is presented. Both methods are ideally suited for fast LBIC scan evaluations.

INTRODUCTION

With decreasing wafer thickness and increasing bulk quality in current cell production lines the determination of the bulk diffusion length L_b and the back surface recombination velocity S_b gains importance for cell process optimization and monitoring in PV industry. One method for obtaining these parameters is based on the internal quantum efficiency (IQE), determined from spectral response and reflectance measurement data.

First calculations of the internal quantum efficiency of solar cells date back to the beginning of solar cell processing [1] with first detailed investigations of the influence of the emitter and the cell thickness to the IQE given in [2,3]. Several approximations for the contribution of the base to the IQE have been suggested [4-8] which result in a linearity between the inverse of the IQE and the light absorption depth. Including recombination of minority carriers at the back side an effective diffusion length L_{eff} can been defined according to Basore [9]:

$$L_{eff.cal} = L_b \cdot \left(s_b \cdot \tanh \frac{W}{L_b} + 1 \right) \Bigg/ \left(s_b + \tanh \frac{W}{L_b} \right) \quad (1)$$

with the normalized back surface recombination velocity $s_b = S_b \cdot L_b / D_b$, the bulk diffusion length L_b and the thickness of the base W (in the following approx. the cell thickness).

The inverse of the internal quantum efficiency was proposed to be approximately [9]:

$$1/IQE(\alpha) = 1 + 1/(\alpha \cdot L_{eff}) \,. \quad (2)$$

The effective diffusion length L_{eff} in eq. 1 is the same that determines the base component of the dark saturation current density as long as potential fluctuations at the collecting junction, e.g. due to inhomogeneous doping profiles at grain boundaries, can be neglected [10].

However the linearity (eq. 2) is not obtained for all cell designs and a fit of equation 2 to IQE-data can result in wrong values for L_{eff} as was shown by some of us [11] by comparing fit results with calculations using the commercially available program IQE1D [12]. Furthermore for cells with considerable loss in the emitter, this has to be taken into account [13] for an accurate theoretical derivation of the IQE at wavelengths up to 900 nm.

The intention of our paper is fourfold:

1. discussion of the limitations of equation 2,
2. introduction of an improved equation for a more accurate determination of L_{eff} (with additional benefit for the simultaneous determination of L_b and S_b),
3. extension of the fit region towards the emitter (which is especially important for future thin cells),
4. suggestion for using these methods for fast evaluation of light beam induced current (LBIC) scans.

THE LIMITATIONS OF EQUATION 2

The general difficulties with eq. 2 are shown in Fig. 1. The inverse IQEs (calculated with IQE1D) in dependence of the light penetration depth normalized with the cell thickness are plotted for different L_b/S_b-pairs. The L_b/S_b-pairs are chosen to yield with eq. 1 the same effective diffusion length equal to the cell thickness (L_{eff}=W). Despite equal L_{eff}-values different inverse IQE curves are obtained in contradiction to eq. 2, which is also plotted in the figure. Deviations to eq. 2 occur for penetration depths much below half the cell thickness, for the two extreme cases (infinite and zero s_b) even down to 0.1 W, which is for a 300 µm thick cell equivalent to λ = 900 nm. Comparing the curves with different internal back side reflection R_b (L_b/W = 1 and s_b = 1) it is shown that the influence of R_b can not be neglected for

$1/\alpha > W/4$. This figure also shows why eq. 2 had been 'successfully' applied by many research groups: it simply gives a good fit for standard 300 µm thick cells with moderate $s_b \approx 1$ and $R_b \approx 0.6$-0.8. With future thin cells including advanced back-side passivation and light-trapping schemes the application of eq. 2 becomes more and more critical.

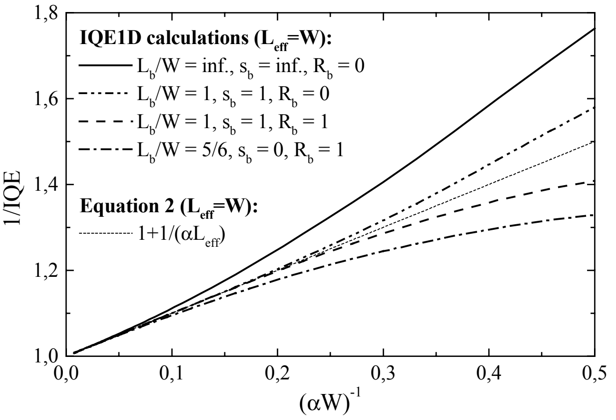

Fig.1: Comparison of eq. 2 with inverse IQEs calculated with IQE1D for 3 different S_b/L_b-pairs, resulting in the same L_{eff} (eq. 1). In addition the influence of no and complete internal backside reflection is shown. Recombination in the emitter is neglected.

IMPROVED APPROXIMATION FOR THE IQE

To overcome the problem stated before we suggest to use the following equation to obtain L_b and L_{eff} simultaneously (or L_b and S_b by using also eq. 1):

$$IQE(\alpha) \approx \frac{1-(\alpha \cdot L_{eff})^{-1}}{1-(\alpha \cdot L_b)^{-2}}. \quad (3)$$

This equation is derived from the contribution of the base [4] assuming a light penetration depth 'large' compared to the emitter thickness and 'small' compared to the cell thickness. Term 'large' depends on various emitter parameters, but can be taken in our case to fulfill $1/\alpha \geq 14$ µm (equivalent to $\lambda \geq 820$). In the following we will see that the term 'small' means $1/\alpha \leq W/4$, which is equivalent to $\lambda \leq 940$ nm for a 200 µm thin cell and $\lambda \leq 960$ nm for a 300 µm thick cell. Larger light penetration depths result in considerable deviations between eq. 3 and the IQE1D-data as shown for a 200 µm thin cell in Fig. 2. With $1/\alpha \leq W/4$ the additional assumption $1/\alpha < L_b$ to be beyond the pole region of eq. 3 is usually fulfilled (or can be fulfilled by adjusting the fit region) and is further discussed in [11, 13].

Determination of L_{eff} – an example

Fig. 2 shows a comparison between numerical data generated by IQE1D, based on the cell parameters as given in Tab. 1, and the results when using eq. 3 for performing a fit on the IQE1D data. For simplification the space charge region width has been set to zero, which will change our results only marginally. Performing a fit with eq. 3 within the wavelength region λ = 820 – 940 nm (equal to $1/\alpha$=14-55µm) results in L_{eff} = 152.1 µm which is in excellent agreement with the calculated value of 152.3 µm obtained by inserting the input parameters into equation 1. The fit also resulted in a bulk diffusion length of 183.2 µm, which is only 8.4% lower than the L_b input parameter.

Using eq. 2 for a fit between $1/\alpha$= 14-55 µm on the IQE1D data results with L_{eff} = 135.6 µm in an 11% lower value than the calculated $L_{eff.cal}$. This was an example where the effective diffusion length differed from the bulk diffusion length (152.3 µm vs. 200 µm). In the following section it is shown that this condition limits the application of eq. 2, whereas eq. 3 results in a considerable improved accuracy in the determination of L_{eff} for a large parameter field.

Table 1: Parameters of the solar cells used in the IQE1D. Internal back side reflection R_b = 0.9 (= 90%).

region	structural and electrical cell parameters: width of regions	diffusion coefficient	diffusion length	Surf. recomb. velocity
emitter	0.4 µm	4 cm²/s	1 µm	1E3 cm/s
base	199.6 µm	32.92 cm²/s	200 µm	1E6 cm/s

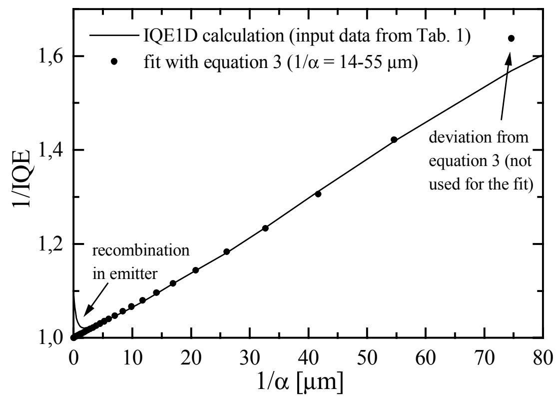

Fig. 2: The inverse of the IQE in dependence on the light penetration depth $1/\alpha$ calculated by IQE1D (line) in comparison with equation 3 (circles).

Influence of L_b and S_b on the determination of L_{eff}

The advantage of eq. 3 will be shown in the following by calculating the IQEs with IQE1D for several parameter sets L_b, S_b and the other parameters given in Tab. 1. The effective diffusion length is either calculated from the input parameters using eq. 1 ($L_{eff.cal}$) or obtained by a fit with eq. 2 or eq. 3 ($L_{eff.fit}$). The influence of L_b/W on the relative error of the effective diffusion length is given in Fig. 3a, showing that eq. 3 is considerable more accurate in the determination of L_{eff} than eq. 2. Equation 2 is limited to small diffusion lengths ($L_b << W$). Fig. 3a is also an example where equation 2 is not good for the determination of L_{eff} even for L_b being a factor 2.5 larger than the cell thickness. For the calculations s_b = 10 was chosen. Varying s_b and keeping L_b = 300 µm fixed results in Fig. 3b, showing that only for $0.75 < s_b < 2$ (abbreviated in the following as $s_b \approx 1$) equation 2 results in a good approximation. Similar graphs have been obtained for bulk diffusion lengths and cell thicknesses between 100 and 500 µm, proving that a considerably increased accuracy in the determination of L_{eff} is obtained by using eq. 3 instead of eq. 2.

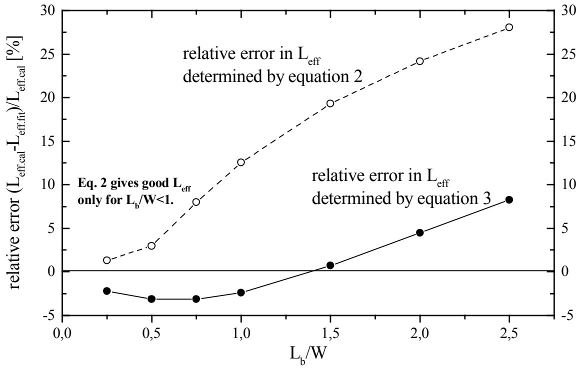

Fig. 3a: Error in L_{eff} determined by a fit with eq. 3 as compared to $L_{eff.cal}$ calculated with eq. 1 as a function of L_b/W. For the calculation s_b = 10 and W = 200 µm was chosen. The dashed curve belongs to the error in L_{eff} when using eq. 2.

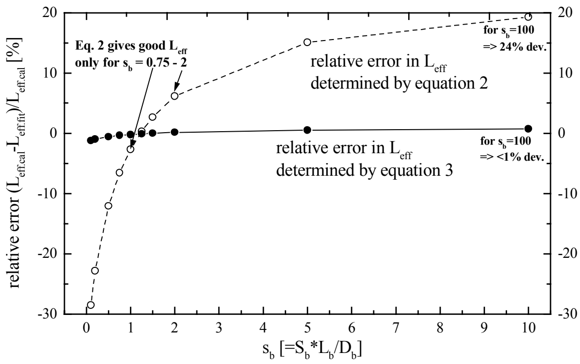

Fig. 3b: Error in L_{eff} determined by a fit with eq. 3 as compared to $L_{eff.cal}$ calculated with eq. 1 as a function of s_b. For the calculation L_b = 300 µm and W = 200 µm was chosen. The dashed curve belongs to the error in L_{eff} when using eq. 2.

From equation 3 back to equation 2

For the case $L_{eff} \approx L_b$ equation 3 reduces to equation 2. From eq. 1 follows that the approximations of either $L_b << W$ or $s_b \approx 1$ as stated before can be combined in the approximation $L_{eff} \approx L_b$. From this and the previous section follows that the application of eq. 2 is restricted to the approximation $L_{eff} \approx L_b$.

SEPARATION OF L_b AND S_b

The possibilities for a separation of L_b and S_b are shown in Tab. 2. Various L_b/S_b-pairs were taken as input parameters for IQE1D calculations and L_{eff}–values obtained by using eq. 1-3 as outlined previously. From a fit with eq. 3 also L_b was obtained and S_b calculated using again eq. 1. The comparison of the gray columns with the column for eq. 2 proves again that with eq. 3 the value L_{eff} is obtained with a considerable higher accuracy than using eq. 2.

From the data given in this table the following statements on the separation of L_b and S_b can be made:

- **A high accuracy on L_b** is given in case of **1. L_b > W** only if S_b is small (L_b =300 µm => S_b < 2000 cm/s, L_b = 500 µm => S_b < 1000 cm/s) and **2. $L_b \le W$** for all S_b–values.
- **Accuracy on S_b**: The larger L_b/W the better the accuracy for low S_b-values and the worse for high S_b-values (for L_b = 300 µm and W = 200 µm a good agreement is found for S_b–values between 100 and 2000 cm/s),
  L_b << W results only in a low sensitivity on S_b (for L_b =100 µm, W = 200 µm and S_b = 1e3 cm/s, S_b obtained by a fit is increased by nearly a factor of 2).

Tab. 2: A comparison of the L_{eff}-values, obtained by eq. 1 using the input parameters, by a fit with eq. 2 to the simulated IQE and, respectively, by a fit with eq. 3. The bold figures belong to cases where the error between fit result and $L_{eff.cal}$ was larger than 10%. The cell thickness W was 200 µm for all rows except the last one with W = 500 µm*. For high back side recombination velocities the uncertainty was to large to determine S_b**.

L_b [µm]	S_b [cm/s]	$L_{eff.cal}$ [µm] eq. 1	L_{eff} [µm] eq. 2	L_{eff} [µm] eq. 3	L_b [µm] eq. 3	S_b [cm/s] eq. 1+3
500	100	996	**1230**	979	516	125
500	1000	415	405	410	423	841
300	100	469	**606**	475	315	169
300	1000	307	320	308	290	891
300	2000	257	244	257	277	1636
300	5000	213	**183**	212	261	3543
300	1e6	175	**132**	173	241	**
200	100	255	**321**	261	211	263
200	1000	214	231	217	203	999
200	1e6	152	**136**	152	183	**
100	1000	102	108	105	104	1903
100	1e6	96	89	98	101	**
100*	1e6	100	99	103	105	**

EXPERIMENTAL RESULTS

IQE-data has been obtained from SR- and R-measurements of three mc-Si cells, which have been processed similarly, but were made out of material with different quality, resulting in comparable S_b–values but different L_b-values, as seen in Tab. 3. For increasing L_{eff}–values the differences between the two evaluation methods (eq. 2 and 3) grow, showing that the more accurate equation 3 has to be taken to determine L_{eff}.

The errors in L_b and S_b show that a high measurement accuracy is needed for the parameter separation.

Tab. 3: Experimentally determined L_{eff} by eq. 2 and L_{eff}, L_b and S_b by our proposed method for three Si cells.

Cell no.	L_{eff} [µm] eq. 2	L_{eff} [µm] eq. 3	L_b [µm] eq. 3	S_b [cm/s] eq. 1 + 3
1	214	226 (±6)	251 (±25)	2206 (±463)
2	189	198 (±4)	207 (±14)	2154 (±458)
3	138	145 (±14)	150 (±24)	3514 (±2412)

INCLUDING THE LOSS IN THE EMITTER

With decreasing cell thickness the fit region of eq. 3 should be shifted towards the emitter region. In case of low quality emitters also recombination in the emitter has to be taken into account, therefore we will shortly outline our recent work on the emitter contribution to the IQE.
Including the emitter into eq. 3 can be made by describing the emitter with a dead layer region of thickness *d* as presented in the following equation:

$$IQE(\alpha) \approx e^{-\alpha \cdot d} \frac{1-(\alpha \cdot L_{eff})^{-1}}{1-(\alpha \cdot L_b)^{-2}} . \qquad (4)$$

Fig. 4 shows a calculated IQE with S_e = 1e6 cm/s and the other parameters given in Tab. 1. Even for this extreme case eq. 4 holds valid down to $1/\alpha$ = 1 µm, or more generally formulated down to 1.5-3 times the emitter thickness, which was also stated in earlier work of one of the authors [13].

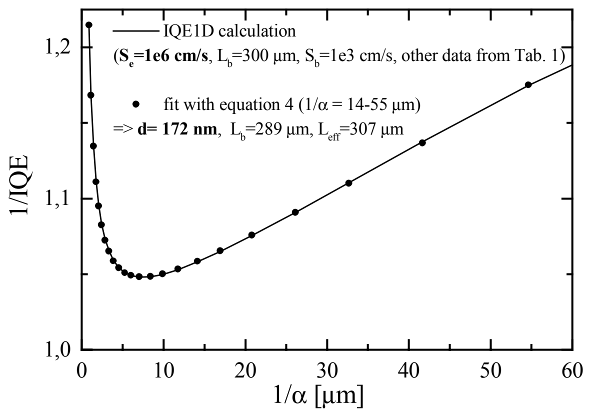

Fig. 4: Inverse IQE calculated by IQE1D and fitted with equation 4.
Excellent fits with eq. 4 to IQE1D simulations have been obtained for various combinations of S_e, L_e and w_e. Furthermore the validity of eq. 4 has been shown for various emitter profiles (homogeneous, error and exponential profiles) representing emitter sheet resistivities between 10 and 200 Ohm/sqr using the simulation package PC1D.

CONCLUSION

By calculating IQEs with the software program IQE1D and experimentally determined IQE-data it has been shown that the linear approximation for the inverse IQE results only in a good fit of the effective diffusion length L_{eff} for the case $L_{eff} \approx L_b$. The discrepancy with the linear approximated inverse IQE equation is solved by the presentation of an improved equation, making it possible to obtain both recombination parameters, L_b and L_{eff} simultaneously (or alternatively L_b and S_b), from a fit on the IQE for wavelengths between 820 nm and a wavelength corresponding to a light penetration depth equal to 1/4 of the cell thickness. Using this equation instead of the linear approximation results in at least a factor of 2 improved accuracy on the determination of L_{eff}, therefore also increasing the accuracy of L_b and S_b. In addition an equation incl. the loss in the emitter has been presented. The simplicity of both methods make them suitable for fast LBIC scan evaluations, from which detailed information on the spatial distribution of L_b and S_b for advanced thin mc-Si solar cells can be obtained. Experiments will be carried out to determine the requirements on the measurement accuracy.

ACKNOWLEDGEMENTS

We like to thank D. Sontag for supplying the solar cells.

REFERENCES

[1] W.G. Pfann and W. Van Roosbroeck, J. Appl. Phys. **25**, 1954, p. 1422-1434.
[2] M. Wolf, M. Prince, Proc. of the IEEE **18**, 1958, p. 583
[3] M. Wolf, Proc. IRE **48**, 1960, p. 1246-1263.
[4] J.H. Reynolds and A. Meulenberg, Jr., J. Appl. Phys. **45(6)**, 1974, p. 2582-2592.
[5] M.A. Green, A.W. Blakers and C.R. Osterwald, J. Appl. Phys. **58(11)**, 1985, p. 4402-4408.
[6] J. Dugas and J. Oualid, Solar Cells **20**, 1987, p. 167.
[7] P.A. Basore, IEEE Tr. El. Devics, **37(2)**, 1990, p. 337.
[8] N. Bordin, L. Kreinin, N. Eisenberg, to be published in proceedings of the 16th EC PVSEC, Glasgow, GB.
[9] P.A. Basore, Proceedings of the 23rd IEEE Photovoltaics Spec. Conf., New York, 1993, pp. 147.
[10] R. Brendel, U. Rau, J. Appl. Phys. **85**, 1999, p. 3634.
[11] S. Keller, M. Spiegel, P. Fath, G. Willeke and E. Bucher, IEEE Trans. Electron Dev **45(7)**, 1998, p. 1569.
[12] R. Brendel, M. Hirsch, R. Plieninger and J.H. Werner, IEEE Trans. Electron Dev **43(7)**, 1996, pp. 1104.
[13] M. Spiegel, thesis, University of Konstanz, 1998.